Uludağ University Journal of The Faculty of Engineering, Vol. 23, No. 3, 2018 RESEARCH

DOI:10.17482/uumfd.408901

ANALYSIS OF SURFACE PLASMON RESONANCE SENSING BASED ON PHASE-DETECTION IN THE INFRARED RANGE

Aykut KOÇ *

Received: 22.03.2018; revised: 26.09.2018; accepted: 17.10.2018

Abstract: Using phase detection in Surface Plasmon Resonance (SPR) sensing has potential improvements to the conventional intensity detection based SPR. Other than the phase detection and intensity detection based SPR in the visible range of the spectrum, employing SPR sensing principles in the infrared range by the use of silicon has also some promising advantages. Combining these two, in this paper, phase detection-based SPR sensing in the infrared range is studied using a mathematical model and numerical simulations. The results are compared with the results obtained by the simulations in the visible range. Performance improvements are noted by the use phase detection in the infrared range.

Keywords: Surface Plasmon Resonance, Optoelectronics, Photonics, Optics

Faz Tespitine Dayalı Yüzey Plazmon Resonans Tabanlı Algılamanın Kızılötesi Bantta Analizi

Öz: Yüzey Plazmon Rezonansı (YPR) tabanlı algılamada geleneksel olarak kullanılan ışık şiddeti tespiti yerine faz tespitine dayanan bir yöntemin kullanılmasının önemli avantajları vardır. Bununla beraber ışık spektrumunun görünür aralığının yerine silikon kullanımıyla kızılötesi aralığında YPR tabanlı algılama yapılması da bazı umut verici avantajlara sahiptir. Bu çalışmada, faz algılamaya dayalı SPR algılamanın kızılötesi aralıkta ışık kullanımıyla birleştirilmesinin yaratacağı performans artışları matematiksel bir model ve sayısal benzetim yöntemleri kullanılarak incelenmiştir. Elde edilen sonuçlar, görünür banttaki benzetimlerden elde edilen sonuçlarla karşılaştırılmış ve kızılötesi bantta faz ölçümü tabanlı yaklaşımın daha yüksek performans verdiği gösterilmiştir.

Anahtar Kelimeler: Yüzey Plazmon Resonansı, Optoelektronik, Fotonik, Optik

1. INTRODUCTION

Surface Plasmon Resonance (SPR) optical sensing, which uses the resonance of surface plasma waves present under special conditions at the interface between a dielectric and a thin metal layer, is a powerful tool to monitor physical, chemical and bio-chemical processes, (Homola et al., 1999) (Nguyen et al., 2015) (Tang et al., 2010), (Daghestani et al., 2010). The principles of surface plasmons are studied in great detail by (Raether, 1988). Biosensors based on SPR methods have also a very promising potential in real-time and label-free monitoring of biomolecular interactions as well as several other advantages (see (Homola et al., 1999), (Homola, 2003), (Nguyen et al., 2015) and the references therein).

The method used in excitation of the surface plasmon, the interrogation (detection) method and the wavelength of the light used in the system are of crucial importance since they directly affect the implementation and the performance of the system. A configuration named Kretschmann-Raether attenuated total reflection (ATR) (or just Kretschmann configuration),

* ASELSAN Research Center, Ankara 06370, Turkey
Corresponding Author: Aykut Koç (aykutkoc@aselsan.com.tr)

(Kretschmann and Raether, 1968), is widely adopted as the method used for most of the SPR-based sensing systems. The advantages of this method arise in its easy construction and in its allowance of the light to be sent from the interrogation side but not through the sample layer.

SPR occurs subject to certain conditions which can be found in almost all sources on the topic such as (Homola et al., 1999), (Homola, 2003). When SPR conditions are satisfied, the incident light is coupled to the surface plasma wave. Due to this coupling there occur two changes in the reflected light: a dip in the intensity and a phase anomaly (an abrupt change in the phase) of the reflected light. As the interrogation method, detecting the dip in the intensity is regarded as the conventional method and is studied by several authors, (Nylander et al., 1982), (Liedberg et al., 1983), (Vidal et al., 1993). Detecting the phase anomaly is offered as a method with potential improvements in the several performance measures. Under certain conditions and fixed wavelength and incidence angle, the phase of the complex amplitude reflectivity abruptly changes around a certain value for sample layer relative dielectric constant or around a dynamic range. Since this phase change is so steep, it can yield an improved sensitivity. Several considerations of phase detection can be found in the literature, (Kabashin and Nikitin, 1997), (Wu et al., 2004), (Kabashin and Nikitin, 1998), (Wu and Pao, 2004), (Kochergin et al., 2012). In these works, it is proposed that by employing the phase detection, an improvement around 3 orders of magnitude can be achievable in the sensitivity of the detection. In (Wu et al., 2004), Wu et al. proposes a differential phase-sensitive SPR system that achieves a sensitivity limit of 5.5×10^{-8} refractive-index units per 0.01^0 phase change. However, a very recent study, (Ran and Lipson, 2006), compares the sensitivity performances of intensity and phase detection schemes. It claims that the phase detection does not yield better results than the intensity detection but yields results in the same order of magnitudes with the intensity method. The argument of this study is that phase cannot be measured directly but can only be measured by using interferometric methods in which the only optically measurable quantity (intensity) is inevitably used. Thus, the ultimate limits are governed by photon statistics.

Regarding the wavelength of light that is used within the system, we have two options. Mainly, the light with the wavelength in the visible range is used within most of the SPR sensing systems. Accordingly, a glass prism, which is transparent to this visible range, is also used in the Kretschmann configuration. Secondly, some research to understand the SPR principles and other related behavior in the infrared, especially near-infrared, are also reported, (Patskovsky et al., 2003a, (Patskovsky et al., 2004), (Patskovsky et al., 2003b), (Lirtsman et al., 2008), (Cleary et al., 2010a), (Cleary et al., 2010b), (Soref et al., 2008) and (Cleary et al., 2010c). Using infrared light requires the use of silicon, which is transparent in the infrared range, as the prism material instead of the glass. Main motivation in using the infrared light and consequently using silicon is twofold. First, sensing performance, especially in sensitivity and resolution, is improved. Secondly, using silicon, for which integrated processing and manufacturing techniques and facilities have been already well established, can lead to the miniaturization and integration of SPR sensors. A study on some properties and characteristics of SPR sensing in the infrared range including the SPR curves, effects of wavelength and metallic layer thickness is presented in (Patskovsky et al., 2003). Further addressing of the topic is also studied in (Patskovsky et al., 2004), (Patskovsky et al., 2003). These works consider only the intensity interrogation as a detection method.

Motivated by combining the advantages of phase detection and infrared light-based SPR sensing using silicon, this paper reports behavior of phase detection-based SPR sensing in infrared range by use of a mathematical model and numerical simulatios. The comparisons with SPR sensing in visible range to investigate the superiority of using infrared light over visible light is also reported. SPR sensing system is studied in the Kretschmann configuration that consists of 3-layered structure of prism-metal-sample. The mathematical model to represent this structure is based on the Fresnel equations. The paper is organized as follows: firstly, the mathematical model is presented, then the results of the numerical simulations using this model

as well as the optimization issues of metal thickness are reported for both infrared and the visible light range. The comparison of results are reported and a future proposal is given for improving the metal layer thickness optimization. Then the paper concludes with a final discussion.

2. THE MODEL AND THEORY

The SPR system modelled in this paper uses Kretschmann configuration to excite the surface plasmons. This three-layered configuration is composed of a prism layer, a metal layer and a sample layer as seen in Fig. 1.

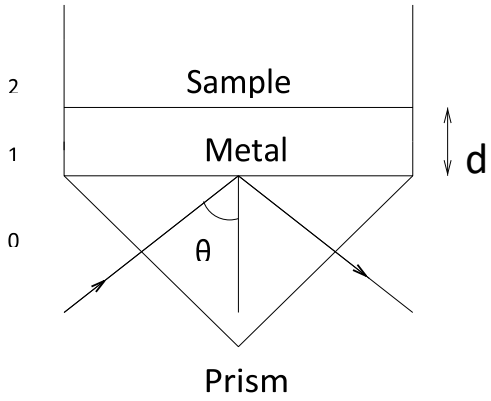

Figure 1:
The SPR Kretschmann Configuration

Fresnel equations for three-layered structure and for a TM-polarized light beam is used below to represent the SPR system by expressing the complex amplitude reflection coefficients between corresponding media as $r_{0,1}$, $r_{1,2}$ and $r_{0,2}$, (Hecht, 1987). Subscripts 0, 1 and 2 stand for prism, metal and sample layers, respectively.

$$r_{0,2} = \frac{r_{0,1}+r_{1,2}e^{2jdk_{z1}}}{1+r_{0,1}r_{1,2}e^{2jdk_{z1}}} \tag{1}$$

$$r_{0,1} = \frac{x_1-x_0}{x_1+x_0} \tag{2}$$

$$r_{1,2} = \frac{x_2-x_1}{x_2+x_1} \tag{3}$$

where

$$x_0 = \frac{\varepsilon_0}{k_{z0}}, \qquad x_1 = \frac{\varepsilon_1}{k_{z1}}, \qquad x_2 = \frac{\varepsilon_2}{k_{z2}} \tag{4}$$

The corresponding wavenumbers in the above equations for the transmitted light in the three mediums are given below:

$$k_{z0} = \sqrt{\left(\frac{\omega}{c}\right)^2 \varepsilon_0 - k_{0x}^2} \tag{5}$$

$$k_{z1} = \sqrt{\left(\frac{\omega}{c}\right)^2 \varepsilon_1 - k_{0x}^2} \tag{6}$$

$$k_{z2} = \sqrt{\left(\frac{\omega}{c}\right)^2 \varepsilon_2 - k_{0x}^2} \tag{7}$$

$$k_{0x} = \left(\frac{\omega}{c}\right)\sqrt{\varepsilon_0}\sin\theta. \tag{8}$$

Here, k_{0x} is the wave number of the incident beam on the surface and θ is the angle of incidence. ε_0, ε_1, and ε_2 stand for relative dielectric constants for prism, metal layer and sample, respectively. d is the thickness of the metallic layer. ω is the angular frequency of the beam and c is the speed of light in vacuum. The prism material is assumed to be silicon when working with infrared light. It is assumed to be BK7 glass when working with visible light. The metal layer is assumed to be Silver (Ag). Optical properties of silicon is obtained from (Virginia Semiconductor) and those of silver is obtained from (Lide, 1992). The relative dielectric constant of BK-7 glass is taken as ε_0 = 2.2957 at the wavelength of interest.

From the complex amplitude reflection coefficients $r_{0,2}$, the intensity coefficient (or the reflectance) R and the phase shift, Φ, can be obtained as

$$R = \left|r_{0,2}\right|^2 \tag{9}$$

$$\Phi = \mathrm{Arg}\left(r_{0,2}\right). \tag{10}$$

3. RESULTS AT INFRARED LIGHT

To investigate the behavior of SPR sensing at infrared range, a silicon prism coated by a silver metallic layer is used in the Kretschmann configuration. The reflectance R and phase shift Φ of the SPR sensing system are investigated by using an infrared light beam of λ = 1240 nm. At this wavelength, the complex dielectric constant of silver is ε_1= −81.4625 + j5.0568 and that of silicon is ε_0 = 12.37275. For all of the numerical simulations reported for infrared range in this paper, the above values are used.

First of all, the SPR characteristics of our system and the effects of the thickness of metal layer are investigated. In the Figs. 2 and 3, the intensity (R) and phase (Φ) of the reflected light versus angle of incidence are given for different values of d. The dielectric constant of the sample medium is kept constant.

As seen from Fig. 2 and Fig. 3, the strength of the excitation of the surface plasmon can be monitored by looking at both intensity and phase shifts. When the surface plasmon resonance condition starts to exist, there occurs a dip in the reflectance together with an observation of phase anomaly. The more the system approaches to the SPR conditions, the better incoming beam is coupled to the surface plasmon. Thus, the light is absorbed and the absorbtion lines gets narrower and stronger. Moreover, the phase anomaly gets steeper. Another observation from these figures is that the thickness of the metal layer is a major effect on the SPR behavior. For the above simulations, when d = 5 nm there is almost no resonance effect and the phase change occurs very slowly. When the thickness increases the SPR effect gets stronger. At around d = 40nm the coupling seems to occur completely, the reflectance drops nearly to zero and the phase change becomes entirely abrupt. However, as we keep increasing the thickness, the coupling does not continue to increase but contrarily decrease. Therefore, an optimization of thickness to obtain the full coupling is necessary. Although our ultimate objective is to use the phase anomaly as means of interrogation, one can use the intensity to find the optimum thickness. When the reflectance becomes almost zero at the optimum thickness, the phase behavior becomes optimum for detection purposes, ie. the phase change takes its steepest value.

The change of the optical properties and thus the change in the dielectric constant of the sample layer should be mapped to the change of the SPR conditions. To grasp a general sense of the effects of the dielectric constant of sample layer to the SPR curve, the SPR behavior is plotted for several dynamic ranges of sample layer dielectric constant, ε_s in Fig. 4.

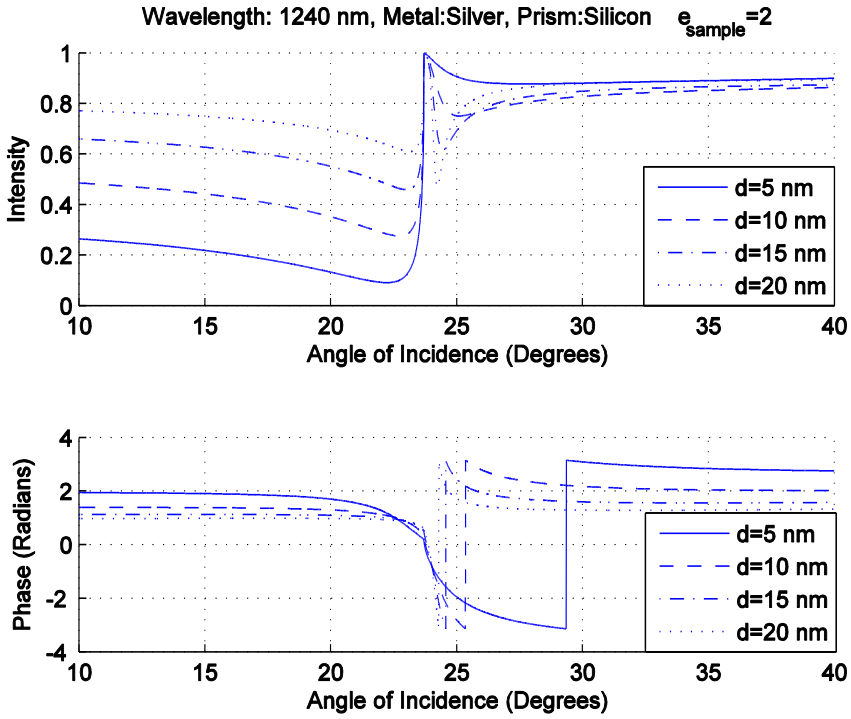

Figure 2:
Intensity and phase shift of reflected light vs. angle of incidence for d = 5 to 20 nm

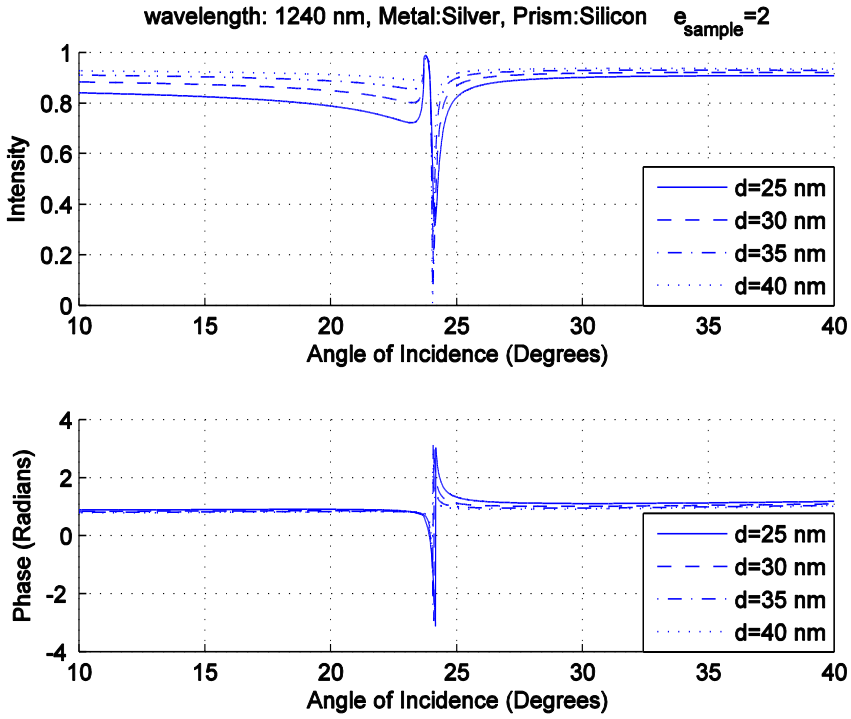

Figure 3:
Intensity and phase shift of reflected light vs. angle of incidence for d= 25 to 40 nm

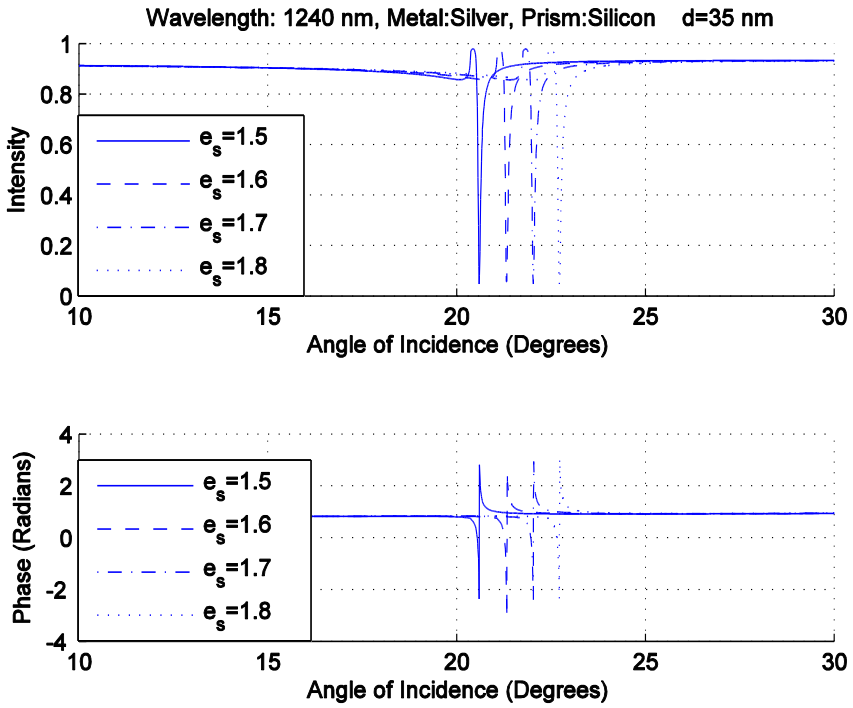

Figure 4:
Intensity and phase shift of reflected light vs. angle of incidence for several ε_s

From this figure we can understand that when the dielectric constant of the sample layer changes, the coupling condition also changes and the angle of incidence necessary for satisfying the SPR condition shifts. Thus, to cover a particular region of interest in sample dielectric constant, the angle of incidence should be set to the corresponding value. Then the phase detection scheme can be employed at this angle of incidence for the particular dynamic range.

The optimization of the metal layer and the optimization of fixed angle of incidence used within the system are of crucial importance. However, this is not a trivial issue. There are two parameters, the metal layer thickness, d and the angle of incidence, θ that need to be concerned. The main obstacle is the fact that the optimal thicknes is different for every angle of incidence. When we optimize the system to use in one particular angle of incidence, we need to use the corresponding optimal value of thickness. However, when we change the operating angle of incidence to use the system to cover another dynamic range of sample dielectric constant, the thickness value is no longer optimal. This means that there is a trade-off between the dynamic range and the sensitivity. To demonstrate this, the thickness is set to 40nm and the SPR curves are plotted for four different angles of incidence 25^0, 40^0, 55^0 and 70^0 in Fig. 5. The thickness is chosen to be 40nm since for a typical sample dielectric constant of $\varepsilon_s \cong 2$, the 40nm value is found to be approximately optimal for angle of incidence equal to 25^0.

As it can be seen from Fig. 5, when the angle of incidence changes considerably, the system starts deviating from the optimal condition. In other words, the phase change gets less steep and reflectance (R) starts increasing. However, optimizing the system around a particular dynamic range of interest can be possible. Then, when we operate within the vicinity of this range, the deviation from optimality can be reduced. This is illustrated in Fig. 6 where SPR curves are plotted for four different values of θ while d is kept constant at 40nm. From Fig. 6, where the SPR dips are zoomed, we can see that for every theta value, the dip occurs at a different ε_s but reflectance is approximately zero, which means that by setting d = 40nm we can achieve optimum coupling.

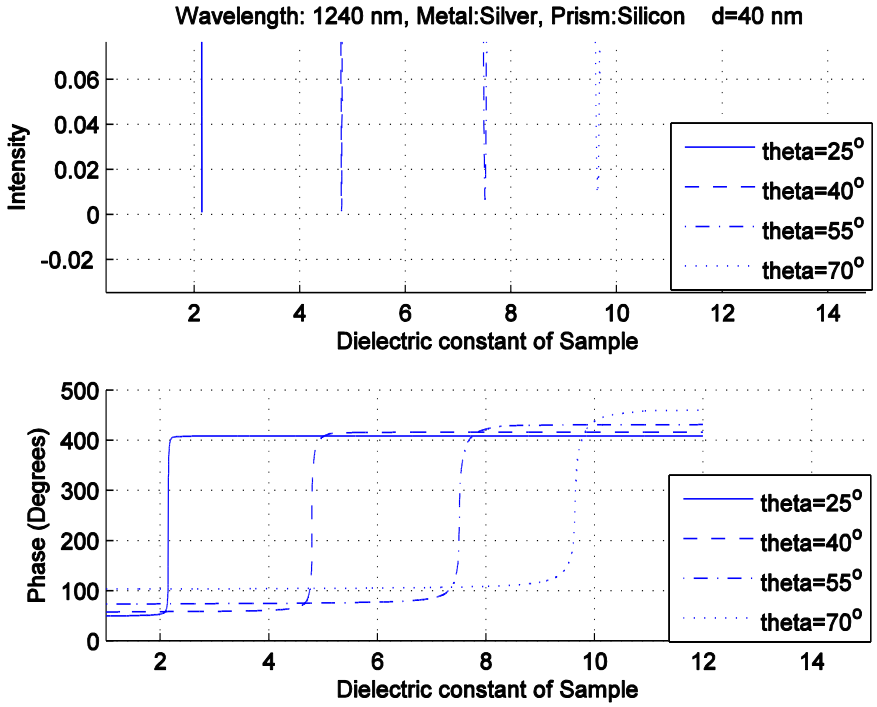

Figure 5:
Intensity and phase shift of reflected light vs. ε_s

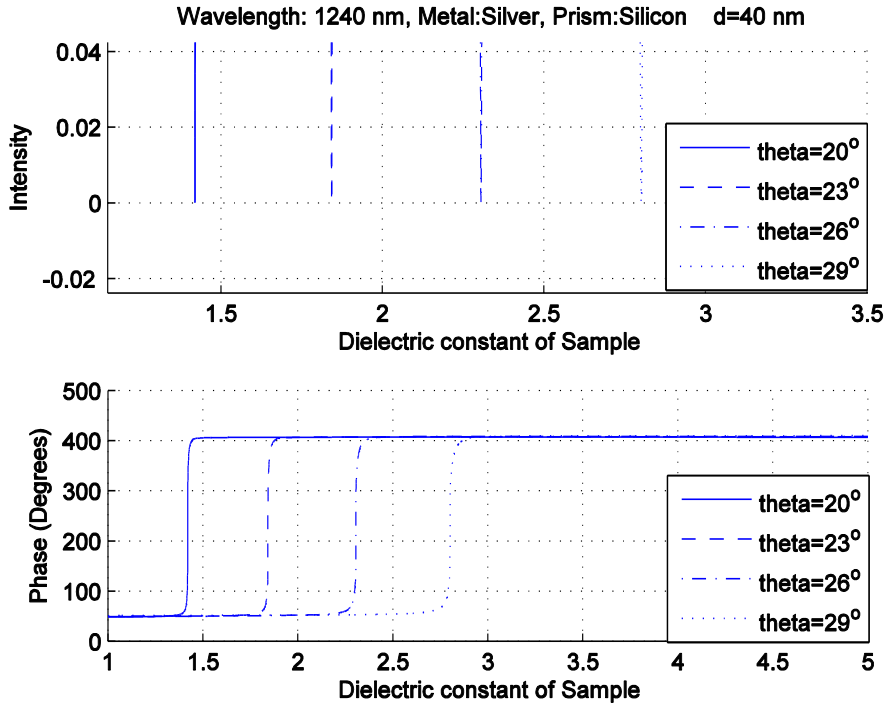

Figure 6:
Intensity and phase shift of reflected light vs. ε_s for several θ, where d = 40nm

In Fig. 7, intensity and phase curves for four different values of d versus sample dielectric constant are seen. Angle of incidence is fixed to $\theta = 22^0$. The intensity plot is given zoomed to better show the behavior. Here, it should be noted that there is an optimal thickness dopt where $35nm < d_{opt} < 45nm$. When the thickness increases towards 40nm, the resonance effect becomes stronger and R decreases together with a sharper change in Φ in positive direction, and finally reaches total coupling to the surface plasmons. However, when d continues to increase and eventually exceeds a certain critical value, the system behavior changes entirely. The coupling amount now starts decreasing, the R value starts increasing and the phase shift Φ changes its behavior from an increase to a decrease as can be seen in Fig. 7. Obviously, the optimal performance can be achieved when there is perfect resonance, ie. R = 0 and Φ is at the position where it experiences its dramatic change in behavior. This point stands for the singularity at the phase character. In other words, as the slope of the phase change around resonance region gets steeper and steeper, at last it can theoretically make a jump with infinite slope. However, it is very hard to achieve such discontinuous phase anomaly in practical implementations.

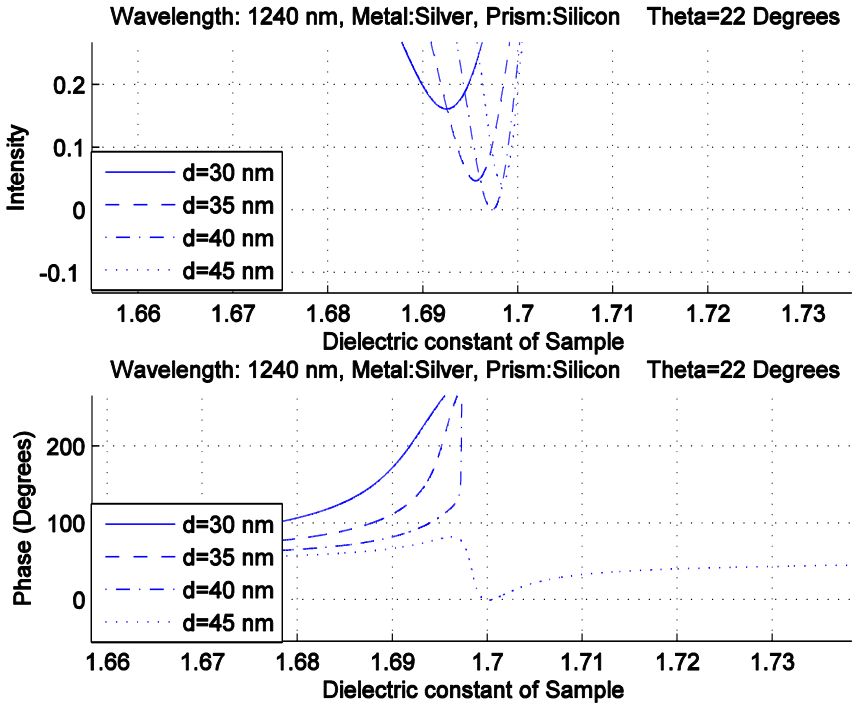

Figure 7:
Intensity and phase shift of reflected light vs. ε_s for several d, where $\theta = 22^0$

To optimize the thickness for a certain angle of incidence and operate close to this optima value, we have already done the coarse tuning and figured out that the optimal thickness is around d = 40nm for $\theta = 22^0$. Now, one can investigate the behavior of the system in more detail around this optimal thickness value of d = 40nm. In Fig. 8, the same analysis as above is given for thickness values of d = 39.5nm, d = 40nm, d = 40.5nm, and d = 41nm. In Fig. 8, the change in the behavior of phase can be seen more explicitly. Reflectance reaches its minimum value and Φ takes its steepest curve at d = 40nm. But, when only for d = 40.5nm, reflectance starts to increase and Φ changes its behavior entirely.

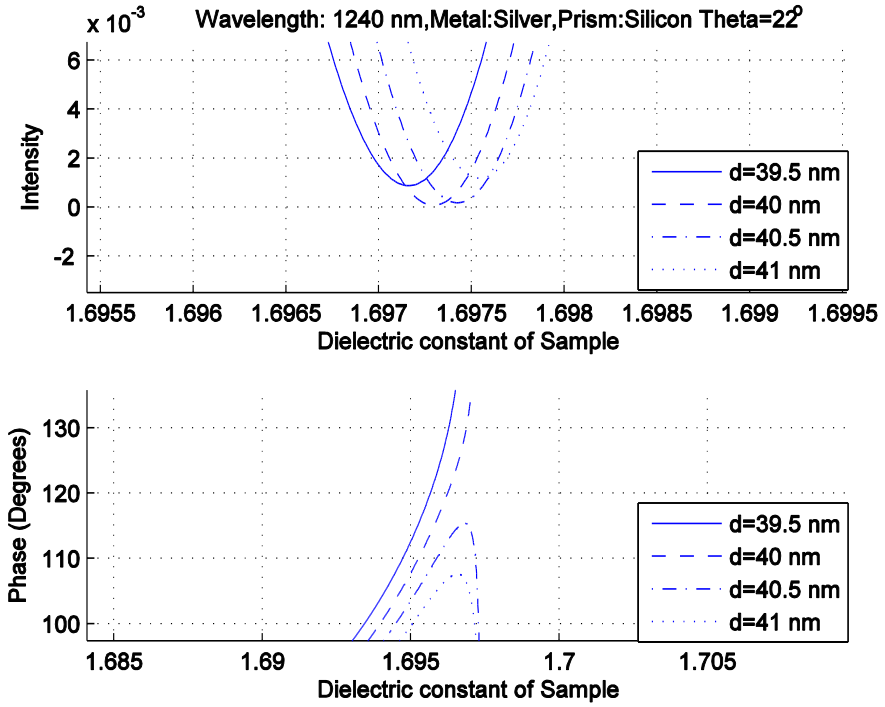

Figure 8:
Intensity and phase shift of reflected light vs. ε_s where $\theta = 22^0$. (A detailed look)

Now another important point should be underlined. The point of singularity in the phase can be perfectly achieved if we have the ability to make the metal layer with the necessary thickness value with perfect accuracy. The degree of accuracy to which we can make the desired thickness directly determines the degree of coupling and also the sensitivity. However, practical issues certainly impose some degree of error between the actual thickness value and the value we want it to be. Therefore, an analysis depending upon the high precision of metal layer thickness does not actually have a practical use.

Lastly, we want to show that the small variations in angle of incidence do not considerably change the SPR performance once it is optimized for a certain angle of incidence. To do this, a similar simulation is done for the case where $\theta = 25^0$ and can be found in Fig. 9. This leads to a situation in which the resonance effect is observed around a bigger ε_s value but the system does not deviate much from the vicinity of full resonance.

As a result, we can state that when we use the infrared light at a wavelength of $\lambda = 1240$ nm, we can set the thickness $d = d_{opt} = 40$nm. We consider this design as almost optimal for infrared case to compare with the visible light case for a particular dynamic range. This will be addressed in the following section.

4. RESULTS AT VISIBLE LIGHT

Similar to the case with infrared light, the Kretschmann configuration is again used to investigate the behavior of SPR sensing at visible range. For this case, a BK-7 glass, which is transparent for visible light, is used as the prism. The coating is same, ie. a silver metallic layer. The reflectance R and phase shift Φ of the SPR sensing system are investigated by using visible light beam of $\lambda = 620$ nm.

At this wavelength, the complex dielectric constant of silver is $\varepsilon_1 = -17.3995 + j2.2572$ and that of BK-7 glass is $\varepsilon_0 = 2.2957$. For the entire numerical simulations reported for visible range in this paper, the above values are used.

As depicted in Fig. 10, the SPR dip moves along the angle of incidence axis when we change the sample layer dielectric constant, as does for the case in infrared range. The plots showing the behavior of SPR curves in the visible range with respect to the gradual change in the thickness of the metal layer that ranges from d = 25 nm to d = 40 nm with 5 nm steps can be seen on Fig. 11.

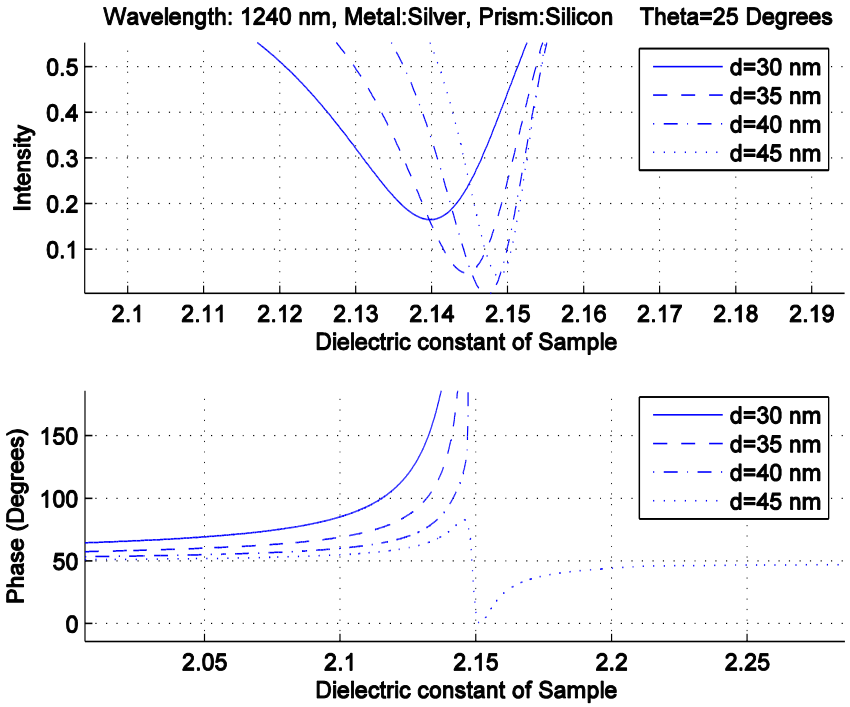

Figure 9:
Intensity and phase shift of reflected light vs. ε_s for several d, where $\theta = 25^0$

The same problem arises in the infrared range is also present in visible range. That is, fully optimizing the thickness is not possible for all angles of incidence. Thus for comparison purposes, we need to approximately determine the d_{opt} for visible range for a particular angle of incidence. From Fig. 11, it is seen that for $\varepsilon_s \cong 2$, d_{opt} is around 37 nm. In Fig. 12, a close look to $d \cong 37$nm region can be seen. Thus we can pick the case for visible range to compare with the infrared range as d equals 37.5 nm and angle of incidence equals 64^0.

To show that changing the angle of incidence in small amounts does not change the value of d_{opt} in a considerable amount, the cases for four different angles of incidence are presented in Fig. 13.

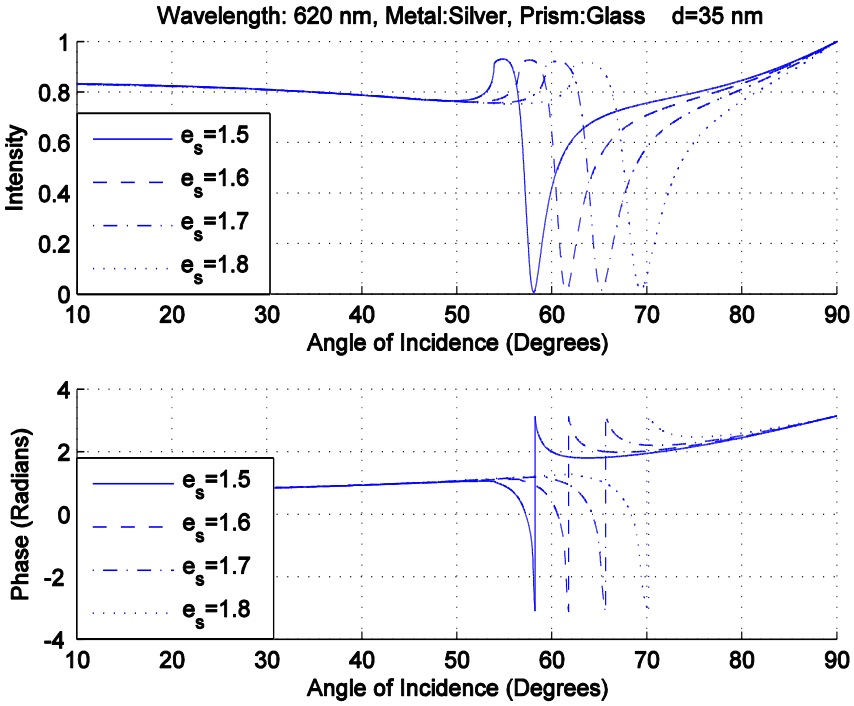

Figure 10:
Intensity and phase shift of reflected light vs. angle of incidence where d = 35nm for several ε_s regions

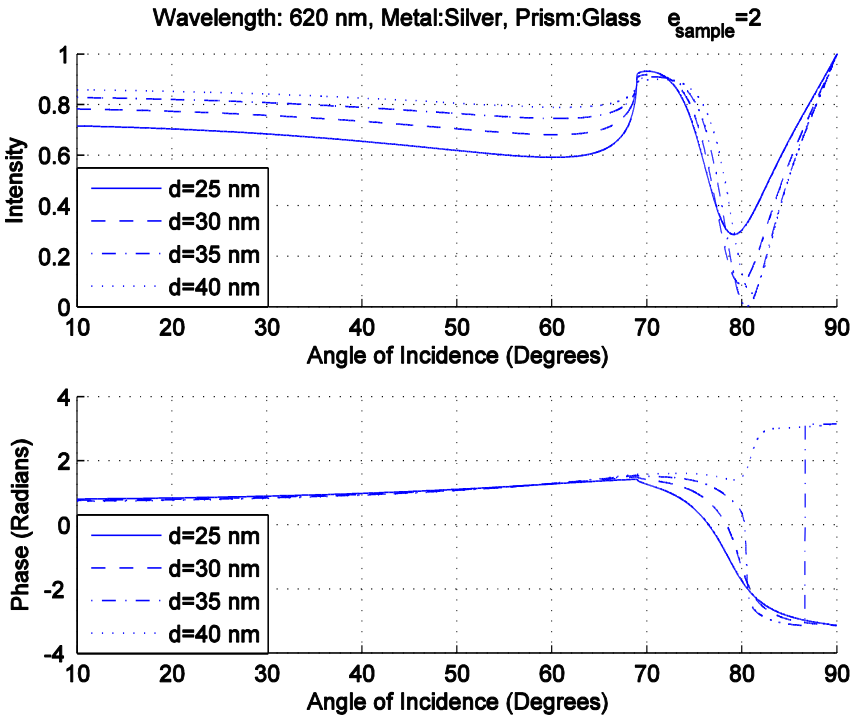

Figure 11:
Intensity and phase shift of reflected light vs. angle of incidence for several d values

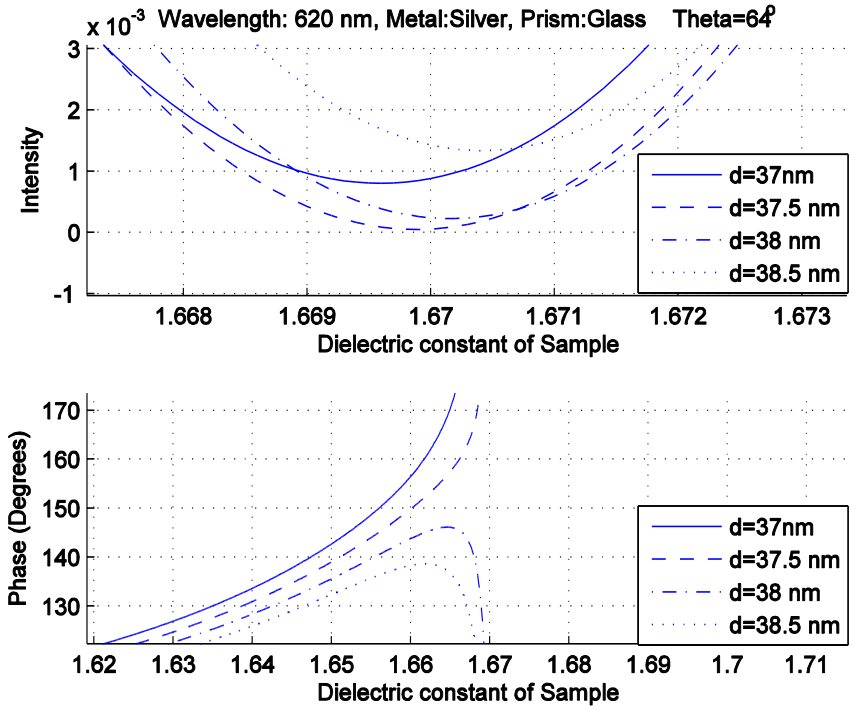

Figure 12:
Intensity and phase shift of reflected light vs. ε_s for several d. $\theta = 64^0$

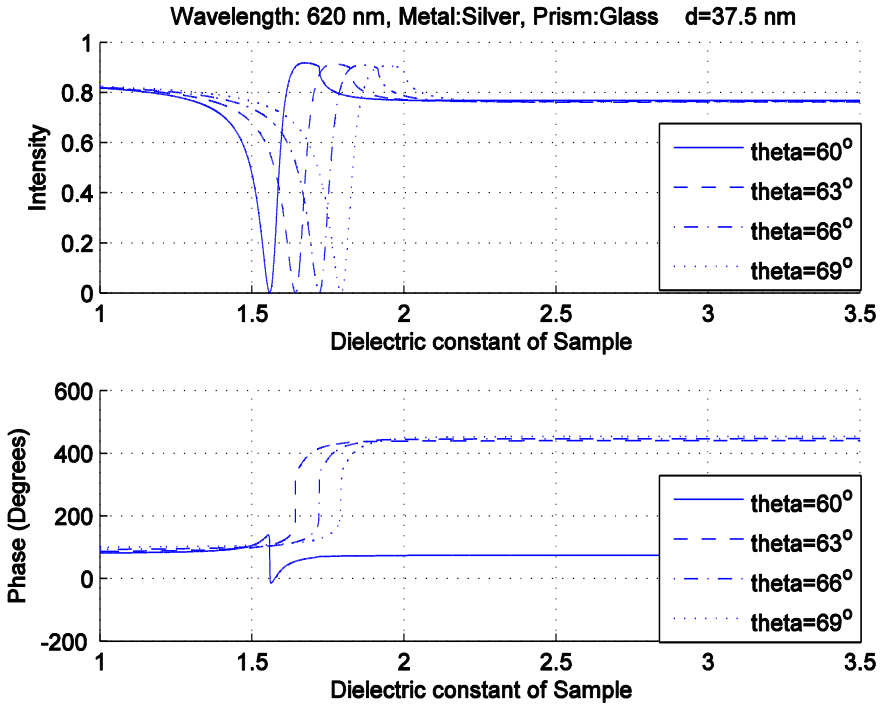

Figure 13:
Intensity and phase shift of reflected light vs. ε_s where d = 35nm for several angles of incidence

5. COMPARISONS

There are several issues to raise when comparing the phase detection schemes between the cases of infrared and visible light. First of all, by the use of infrared light and silicon as a prism material, the integration of SPR sensors can be achieved, which cannot be a case for visible light. This advantage of infrared light is enjoyed by the use of silicon integrated circuit technology.

The second advantage of infrared light upon the visible range in the setting of SPR comes from the fact that the dielectric constant of silicon at the infrared range is much greater than that of glass at visible range. To employ surface plasmon resonance, only the values of sample layer dielectric constant that is smaller than the dielectric constant of prism can be used. The dielectric constant of BK-7 glass at the particular visible wavelength used in this paper is ε_{prism} = 2.2957 and that of silicon at the particular infrared wavelength is ε_{prism} = 12.37275. Therefore, SPR effect can be sustained in visible range for the sample dielectric constant values up to ε_{sample} = 2.2957 while sustained in infrared range up to values of ε_{sample} = 12.37275. Certainly, such values of ε_{sample} greater than 12.37275 can hardly exist in practice. As a result, one can practically cover all possible values for ε_{sample} by using infrared SPR system.

Lastly, sensitivity issue should be discussed. The optimal thicknesses for metal layers for both visible and infrared schemes are approximately obtained for certain angles of incidence. As aforementioned, both of the infrared and visible range schemes can be optimized if we have the ability to set the thickness of the metal layer with very high precision in practical implementations. This should be done for every angles of incidence necessary to cover the dynamic ranges of interest that is to be employed in the interrogation. In other words, we need a continuum of thickness values to correspondingly optimize the continuum of angles of incidence. A proposal for possible future research to overcome this issue will be presented in the following section. However, for the sake of the comparison of visible and infrared schemes, we need to use approximate values that yield near-optimal results at the particular dynamic ranges. Certainly, these dynamic ranges may be different for infrared and visible ranges. However, we can assume that the performance of a particular SPR system, provided that it is properly optimized for each different dynamic ranges individually, does not change significantly from one dynamic range to another. Thus, as we found in the previous sections, we optimize the infrared scheme with d = 40nm and angle of incidence, $\theta = 22^0$ and optimize the visible scheme with d = 37.5nm and $\theta = 64^0$. Then we can compare the both schemes. In Fig. 14, the phase for the both schemes are plotted with respect to the sample dielectric constant in order to illustrate the sensitivity anlysis.

As can be seen from Fig. 14, a small change in the ε_s can lead to very large phase changes within a particular dynamic range. The sensitivity is defined as the smallest change in ε_s that can be detected. Since phase change is the central quantity that is detected, the smallest phase change that can be measured is important. Given that value, the minimum necessary dielectric constant variation of sample which can cause this particular phase shift can be determined. Thus, the minimum dielectric constant change that can be detected can be found. This defines the sensitivity of the system. Regarding the numerical simulations, the sensitivity obtained from infrared range is bigger than that of visible range. This can be perceived from the plot as we note the steeper change in phase for infrared scheme.

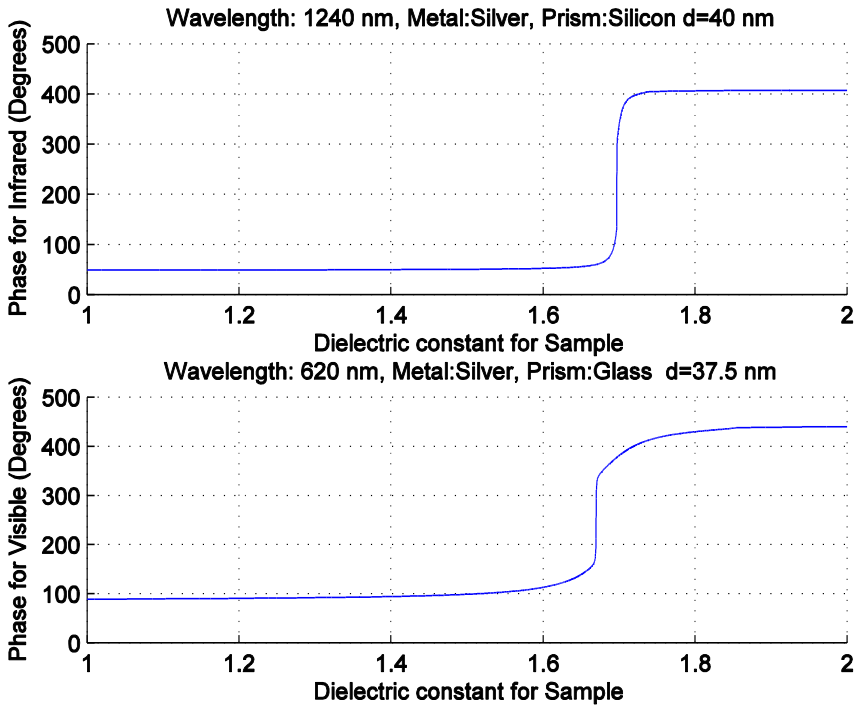

Figure 14:
Phase changes for infrared and visible ranges

6. CONCLUSIONS

In this paper, the basic phase detection characteristics and sensitivity performance comparisons are reported based on numerical simulations. The simulations are performed based on a mathematical model using the Fresnel equations. First, the optimization of both the infrared and visible range schemes are addressed. The optimization of the metal layer thickness is of greater importance. It turns out to be that the thickness optimized to be used in a particular angle of incidence cannot lead to optimized results when used with different angles of incidence. Certainly, this leads to a trade-off between dynamic range and sensitivity. To compare the two schemes, first the systems are optimized for a particular dynamic range individually and then the phase change characteristics are compared. The infrared scheme has more abrupt change in the phase than visible range, leading to bigger values of sensitivity. Another important advantage of the infrared scheme is that it can sustain a more broad dynamic ranges up to ε_s values around 10 while the visible range can only sustain that of around 2. This allows the systems using infrared light can detect target analytes with very high dielectric constants.

REFERENCES

1. J. W. Cleary, G. Medhi, R. E. Peale, W. R. Buchwald, O. Edwards, and I. Oladeji, "Infrared surface plasmon resonance biosensor," Proc. SPIE 767306 (2010). doi: 10.1117/12.852576.

2. J. W. Cleary, R. E. Peale, D. J. Shelton, G. D. Boreman, C. W. Smith, M. Ishigami, R. Soref, A. Drehman, and W.R. Buchwald, "IR permittivities for silicides and doped silicon," J. Opt. Soc. Am. B27, 730-734, (2010). doi: 10.1364/JOSAB.27.000730.

3. J. W. Cleary, G. Medhi, R. E. Peale, and W. R. Buchwald, "Long-wave infrared surface plasmon grating coupler," Appl. Opt. 49, 3102-3110 (2010). doi: 10.1364/AO.49.003102.

4. H. N. Daghestani and B. W. Day, "Theory and Applications of Surface Plasmon Resonance, Resonant Mirror, Resonant Waveguide Grating, and Dual Polarization Interferometry Biosensors", Sensors (Basel, Switzerland). 2010; 10(11):9630-9646. doi: 10.3390/s101109630.

5. E. Hecht, Optics, 2nd ed. Addison-Wesley, 1987.

6. J. Homola, S. S. Yee, and G. Gauglitz, "Surface plasmon resonance sensors: review," Sensors and Actuators B 54, 3-15 (1999). doi: 10.1016/S0925-4005(98)00321-9.

7. J. Homola, "Present and future of surface plasmon resonance biosensors," Anal. Bioanal. Chem. 377, 528-539 (2003). doi. 10.1007/s00216-003-2101-0.

8. A. V. Kabashin, P. I. Nikitin, "Interferometer based on a surface-plasmon resonance for sensor applications," Quan. Elec. 27, 653-654 (1997). doi: 10.1070/QE1997v027n07ABEH001013.

9. A. V. Kabashin, P. I. Nikitin, "Surface plasmon resonance interferometer for bio- and chemical-sensors," Opt. Commun. 150, 5-8 (1998). doi: 10.1016/S0030-4018(97)00726-8.

10. V. E. Kochergin, A. A. Beloglazov, M. V. Valeiko, P. I. Nikitin, "Phase properties of a surface-plasmon resonance from the viewpoint of sensor applications," Quan. Elec. 28, 444-448 (1998). doi: 10.1070/QE1998v028n05ABEH001245.

11. E. Kretschmann and H. Raether, "Radiative decay of non-radiative surface plasmons excited by light," Z. Naturforsch. 23A, 2135-2136 (1968). doi: 10.1515/zna-1968-1247.

12. D. R. Lide eds. "Handbook of Chemistry and Pyhsics," 72nd Ed., CRC Press, 1991-1992.

13. B. Liedberg, C. Nylander, and I. Lundstrom, "Surface plasmons resonance for gas detection and biosensing," Sens. Actuators 4, 299-304 (1983). doi: 10.1016/0250-6874(83)85036-7.

14. V. Lirtsman, M. Golosovsky, and D. Davidov, "Infrared surface plasmon resonance technique for biological studies", Journal of Applied Physics 103, 014702 (2008). doi: 10.1063/1.2828162.

15. H. H. Nguyen, J. Park, S. Kang, and M. Kim, "Surface plasmon resonance: a versatile technique for biosensor applications", Sensors (Basel) 15, (10481–10510) 2015. doi: 10.3390/s150510481.

16. C. Nylander, B. Liedberg, and T. Lind, "Gas detection by means of surface plasmons resonance," Sens. Actuators 3, 79-88 (1982). doi: 10.1016/0250-6874(82)80008-5.

17. Optical Properties of Silicon, Virginia Semiconductor, Inc. www.virginiasemi.com.

18. S. Patskovsky, A. V. Kabashin, M. Meunier, and J. H. T. Luong, "Properties and sensing characteristics of surface-plasmon resonance in infrared light," J. Opt. Soc. Am. A 20, 1644-1650 (2003). doi: 10.1364/JOSAA.20.001644.

19. S. Patskovsky, A. V. Kabashin, M. Meunier, and J. H. T. Luong, "Silicon-based surface plasmon resonance sensing with two surface plasmon polariton modes," Appl. Opt. 42, 6905-6909 (2003). doi: 10.1364/AO.42.006905.

20. S. Patskovsky, A. V. Kabashin, M. Meunier, and J. H. T. Luong, "Near-infrared surface plasmon resonance sensing on a silicon platform," Sens. Actuators B 97, 409-414 (2004). doi: 10.1016/j.snb.2003.09.023.

21. H. Raether, Surface Plasmons on Smooth and Rough Surfaces and on Gratings (Springer-Verlag, Berlin, 1988).

22. B. Ran and S. G. Lipson, "Comparison between sensitivities of phase and intensity detection in surface plasmon resonance," Opt. Express 14, 5641-5650 (2006). doi: 10.1364/OE.14.005641.

23. R. Soref, R. E. Peale and W. Buchwald, "Longwave plasmonics on doped silicon and silicides," Opt. Express 16, 6507-6514 (2008). doi: 10.1364/OE.16.006507.

24. Y. Tang, X. Zeng, and J. Liang, "Surface Plasmon Resonance: An Introduction to a Surface Spectroscopy Technique", Journal of chemical education. 2010; 87(7):742-746. doi: 10.1021/ed100186y.

25. M. M. B. Vidal, R. Lopez, S. Aleggret, J. AlonsoChamarro, I. Garces, J. Mateo, "Determination of probable alcohol yield in musts by means of an SPR optical sensor," Sens. Actuators B 11, 455-459 (1993). doi: 10.1016/0925-4005(93)85287-K.

26. C. Wu and M. Pao, "Sensitivity-tunable optical sensors based on surface plasmon resonance and phase detection," Opt. Express 12, 3509-3514 (2004). doi: 10.1364/OPEX.12.003509.

27. S. Y. Wu, H. P. Ho, W. C. Law, L. Chinlon, and S. K. Kong, "Highly sensitive differential phase-sensitive surface plasmon resonance biosensor based on the MachZehnder configuration," Opt. Lett. 29, 2378-2380 (2004). doi: 10.1364/OL.29.002378.